

Fall 2012

Design of a 4-Seat, General Aviation, Electric Aircraft

Arvindhakshan Rajagopalan Srilatha
San Jose State University

Follow this and additional works at: https://scholarworks.sjsu.edu/etd_theses

Recommended Citation

Rajagopalan Srilatha, Arvindhakshan, "Design of a 4-Seat, General Aviation, Electric Aircraft" (2012). *Master's Theses*. 4248.
DOI: <https://doi.org/10.31979/etd.rss9-mc3k>
https://scholarworks.sjsu.edu/etd_theses/4248

This Thesis is brought to you for free and open access by the Master's Theses and Graduate Research at SJSU ScholarWorks. It has been accepted for inclusion in Master's Theses by an authorized administrator of SJSU ScholarWorks. For more information, please contact scholarworks@sjsu.edu.

DESIGN OF A 4-SEAT, GENERAL AVIATION, ELECTRIC AIRCRAFT

A Thesis

Presented to

The Faculty of the Department of Mechanical and Aerospace Engineering

San José State University

In Partial Fulfillment

of the Requirements for the Degree

Master of Science

by

Arvindhakshan Rajagopalan

December 2012

© 2012

Arvindhakshan Rajagopalan

ALL RIGHTS RESERVED

The Designated Thesis Committee Approves the Thesis Titled

DESIGN OF A 4-SEAT, GENERAL AVIATION, ELECTRIC AIRCRAFT

By

Arvindhakshan Rajagopalan

APPROVED FOR THE DEPARTMENT OF MECHANICAL AND AEROSPACE
ENGINEERING

SAN JOSÉ STATE UNIVERSITY

December 2012

| | |
|---------------------------|--|
| Dr. Nikos Mourtos | Department of Mechanical and Aerospace Engineering |
| Dr. Periklis Papadopoulos | Department of Mechanical and Aerospace Engineering |
| Srikrishna S. Chittur | Aerodynamics Engineer, Brayton Energy |

ABSTRACT

DESIGN OF A 4-SEAT, GENERAL AVIATION, ELECTRIC AIRCRAFT

By Arvindhakshan Rajagopalan

Range and payload of current electric aircraft is limited primarily due to low energy density of batteries. However, recent advances in battery technology promise storage of more than 1 kWh of energy per kilogram of weight in the near future. This kind of energy storage makes possible the design of an electric aircraft comparable to, if not better than existing state-of-the-art general aviation aircraft powered by internal combustion engines. This thesis explores through parametric studies the effect of lift-to-drag ratio, flight speed, and cruise altitude on required thrust power and battery energy and presents the conceptual and preliminary design of a four-seat, general aviation electric aircraft with a takeoff weight of 1750 kg, a range of 800 km, and a cruise speed of 200 km/h. An innovative configuration design will take full advantage of the electric propulsion system, while a Lithium-Polymer battery and a DC brushless motor will provide the power. Advanced aerodynamics will explore the greatest possible extent of laminar flow on the fuselage, the wing, and the empennage surfaces to minimize drag, while advanced composite structures will provide the greatest possible savings on empty weight. The proposed design is intended to be certifiable under current FAR 23 requirements.

ACKNOWLEDGMENTS

This thesis is a true success because of the never ending love and support from my parents, brother, relatives, teachers and friends.

First, I would like to thank Professor Nikos Mourtos for his support and guidance from the first day of my master's degree. His technical knowledge, simplicity, humbleness, and cheerful attitude make him the most respectful person. I feel so proud to get him as my advisor. His advice and support could never be explained by mere words. I am so grateful to him for helping me throughout my master's degree. This thesis would have never been possible without his encouragement and guidance.

Second, I thank my parents and brother for their unconditional love and support, and their endless confidence in me. Every accomplishment in my life would have never been possible without them.

Finally, I would like to thank my relatives and friends who supported me for my education here in the United States. I am currently in this position only because of their blessings and wishes.

TABLE OF CONTENTS

| | |
|--|------|
| LIST OF FIGURES | vii |
| LIST OF TABLES | viii |
| 1.0 INTRODUCTION | 1 |
| 2.0 THE ROLE OF ELECTRIC AIRCRAFT | 2 |
| 3.0 EXISTING ELECTRIC AIRCRAFT DESIGNS | 3 |
| 3.1 ELECTRA ONE | 4 |
| 3.2 YUNEEC E 430..... | 5 |
| 3.3 CRI-CRI | 6 |
| 3.4 PIPISTREL TAURUS G2 | 7 |
| 3.5 PIPISTREL PANTHERA..... | 8 |
| 3.6 ANTARES H3 | 9 |
| 4.0 DESIGN REQUIREMENTS | 10 |
| 5.0 PROPULSION TYPE SELECTION | 10 |
| 5.1 ELECTRIC MOTOR CHARACTERISTICS | 12 |
| 5.2 PROPELLER CHARACTERISTICS | 12 |
| 5.3 BATTERY CHARACTERISTICS..... | 13 |
| 6.0 PRELIMINARY SIZING | 14 |
| 6.1 TAKEOFF WEIGHT ESTIMATION | 14 |
| 6.2 PERFORMANCE SIZING..... | 15 |
| 6.3 SUMMARY OF PERFORMANCE SIZING | 16 |
| 6.4 BATTERY SIZING | 17 |
| 7.0 PRELIMINARY DESIGN | 20 |
| 7.1 FUSELAGE LAYOUT | 20 |
| 7.2 ENGINE SELECTION AND DISPOSITION | 21 |
| 7.3 WING DESIGN..... | 21 |
| 7.4 WEIGHT AND BALANCE ANALYSIS..... | 23 |
| 7.5 LANDING GEAR | 26 |
| 7.6 EMPENNAGE | 26 |
| 7.7 HIGH LIFT DEVICES | 27 |
| 7.8 AIRFOIL SELECTION..... | 28 |
| 7.9 DRAG POLAR..... | 32 |
| 10.0 PRELIMINARY DESIGN LAYOUT | 34 |
| 11.0 CONCLUSION | 35 |
| REFERENCES | 36 |

LIST OF FIGURES

| | |
|--|----|
| Figure 1. Effect of Climate Change and its Consequences..... | 1 |
| Figure 2. Growth in Aviation-Related Pollutants by 2021. | 2 |
| Figure 3. Electra One [15]. | 4 |
| Figure 4. Yuneec E 430 [16]. | 5 |
| Figure 5. Cri-Cri [17]. | 6 |
| Figure 6. Pipistrel Taurus G2 [18]. | 7 |
| Figure 7. Pipistrel Panthra [19]. | 8 |
| Figure 8. Antares H3 [9]. | 9 |
| Figure 9. Performance Sizing Graph. | 15 |
| Figure 10. Fuselage Dimensions. | 20 |
| Figure 11. Nose Mounted Engine..... | 21 |
| Figure 12. Wing specifications..... | 23 |
| Figure 13. Location of Various Components for Estimating the CG Location. | 24 |
| Figure 14. CG Excursion Diagram. | 25 |
| Figure 15. Drag Polar Comparison of Various Naca 6-Series Airfoils. | 29 |
| Figure 16. Lift and Drag Characteristics Comparison of Various Naca 6-Series Airfoils. | 29 |
| Figure 17. Lift-To-Drag Ratio and Pitching Moment Comparison of Various Naca 6-Series Airfoils. | 30 |
| Figure 18. Comparison of the Drag Polars for the Naca 66212 and Naca 65618 Airfoils. | 30 |
| Figure 19. Comparison of the Lift and Drag of the Naca 66212 and Naca 65618 Airfoils. | 31 |
| Figure 20. Comparison of the L/D Ratio and Moment of the Naca 66212 and Naca 65618 Airfoils. .. | 31 |
| Figure 21. Preliminary Design Layout. | 34 |
| Figure 22. Electric Aircraft: Three View..... | 34 |

LIST OF TABLES

| | |
|--|----|
| Table 1. Existing Electric Aircraft..... | 3 |
| Table 2. Electric Aircraft under Research. | 3 |
| Table 3. Electra One Specifications. | 4 |
| Table 4. Yuneec E 430 Specifications. | 5 |
| Table 5. Cri-Cri Specifications..... | 6 |
| Table 6. Pipistrel Taurus G2 Specifications. | 7 |
| Table 7. Pipistrel Panthera Specifications. | 8 |
| Table 8. Antares H3 Specifications. | 9 |
| Table 9. Fuel Cell Specifications..... | 11 |
| Table 10. Battery Specifications..... | 11 |
| Table 11. Comparison of Different Batteries. | 13 |
| Table 12. Summary of Performance Sizing..... | 16 |
| Table 13. Effect of L/D over Thrust Power and Battery Energy. | 18 |
| Table 14. Effect of L/D over Specific Energy and Battery Mass. | 19 |
| Table 15. Estimation of Empty Weight CG. | 24 |
| Table 16. CG Estimation. | 25 |
| Table 17. Lift Coefficient Increments for Various Types of High Lift Devices..... | 27 |
| Table 18. Preliminary Estimates of C_{d0} and e | 32 |
| Table 19. Drag Coefficient and L/D Ratio for Different Aircraft Configurations. | 33 |

1.0 INTRODUCTION

It is now recognized that emission of carbon, nitrogen oxides, halogens, and other products from the burning of aviation fuel contributes to the climatic change we have been experiencing (e.g., ozone layer depletion, air quality degradation) [1]. Furthermore, current airplane engines are noisy. According to GAO Report 2008, aviation emissions contribute about 1% of the air pollution and 2.7% of the US gas emissions. Although these percentages seem small, global air traffic is predicted to increase at a rate of 20% by 2015 and 60% by 2030. Currently, global aircraft emissions produce about 3.5% of the warming generated by human activity [2]. However, if unchecked, by 2021 the emissions will increase up to 90% from the current level [2]. This negative impact on the environment can be reduced by introducing more eco-friendly propulsion systems and suitable airplane designs. One of the steps to achieve eco-aviation is designing an aircraft with an electric propulsion system.

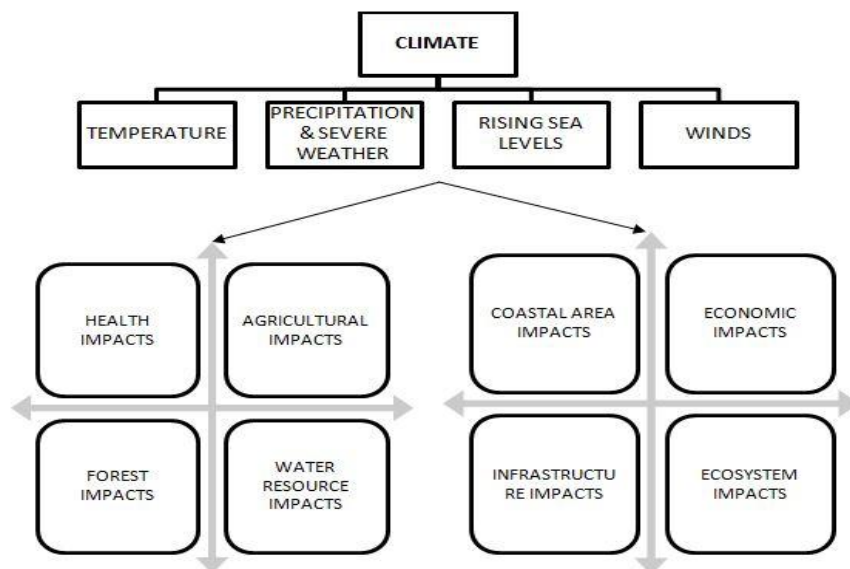


Figure 1. Effect of Climate Change and its Consequences.

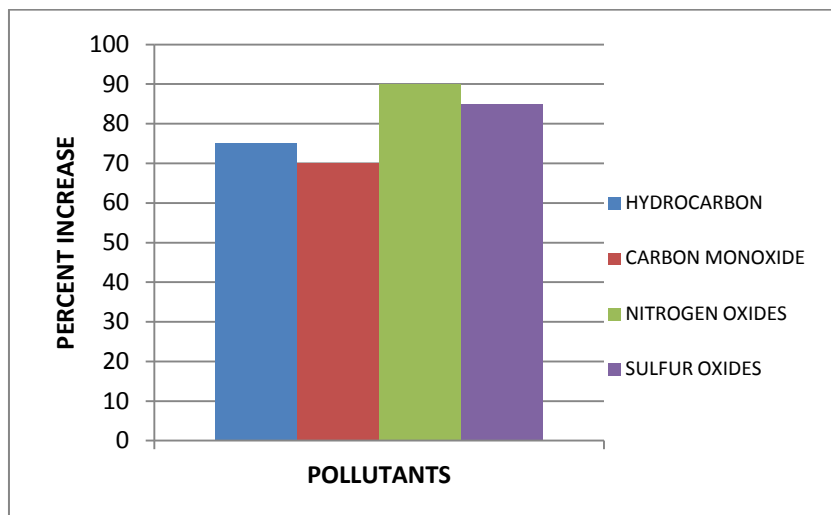


Figure 2. Growth in Aviation-Related Pollutants by 2021.

2.0 THE ROLE OF ELECTRIC AIRCRAFT

The advantages of electric motors (EM) compared to bio fuel are summarized below.

- Very light weight (45 lb for EM compared to 400 lb for ICE)
- More power per unit weight
- More efficient energy conversion (90-95% for EM compared to 20-25% for ICE)
- Improved high altitude performance (higher ceiling as well as airspeed and climb rate)
- Noise reduction
- High reliability and safety
- Lower operating cost (\$5-\$10/h for EM, compared to \$35-\$50/h for ICE)
- Easier maintenance
- Low pollution

3.0 EXISTING ELECTRIC AIRCRAFT DESIGNS

Tables 1 and 2 summarize data on the propulsion types of electric aircraft. Table 1 refers to existing aircraft, whereas Table 2 presents data on aircraft currently under research.

Table 1. Existing Electric Aircraft.

| Company | Name | Type | Propulsion |
|-----------|-------------------|------------|--------------------------------|
| PC Aero | Electra One | 1 - Seat | Electric Motor + Li Po Battery |
| Yuneec | E 430 | 2 - Seat | Electric Motor + Li Po Battery |
| EADS | Cri-Cri | 1 – Seat | Electric Motor + Li Po Battery |
| Pipistrel | Taurus Electro G2 | 2 – Seat | Electric Motor |
| Boeing | ----- | 1 – Seat | Electric Motor |
| Sikorsky | Firefly | Helicopter | Electric Motor |
| Pipistrel | Panthera | 4 - Seat | Electric Motor |

Table 2. Electric Aircraft under Research.

| Company | Name | Type | Propulsion |
|----------------|-----------|--------|--------------------------------|
| Lange Aviation | Antares 3 | UAV | Electric Motor + Fuel Cell |
| Yuneec | E 1000 | 4-Seat | Electric Motor + Li Po Battery |
| Flight Design | ----- | 4-Seat | Electric Motor + Ice |

Figures 3-8 represent the existing electric aircraft while the tables 3-8 show the performance characteristics and specifications of the aircraft [6 - 9].

3.1 ELECTRA ONE

The design of Electra One is shown in Figure 3. The specifications of the aircraft are given in Table 3.



Figure 3. Electra One [15].

Table 3. Electra One Specifications.

| Power System | Electric Motor (Li-Polymer Battery) |
|----------------------|--|
| Number of Seats | 1 |
| Maximum Weight | 300 kg |
| Maximum Engine Power | 16 KW |
| Maximum Range | 400 Km |
| Maximum Endurance | 3 hours |

3.2 YUNEEC E 430

The design of Yuneec E 430 is shown in Figure 4. The specifications of the aircraft are given in Table 4.



Figure 4. Yuneec E 430 [16].

Table 4. Yuneec E 430 Specifications.

| | |
|----------------------|--|
| Power System | Electric Motor (Li-Polymer Battery) |
| Number of Seats | 2 |
| Maximum Weight | 430 kg |
| Maximum Engine Power | 40 KW |
| Maximum Endurance | 2 Hours |

3.3 CRI-CRI

The design of Cri-Cri is shown in Figure 5. The specifications of the aircraft are given in Table 5.



Figure 5. Cri-Cri [17].

Table 5. Cri-Cri Specifications.

| | |
|----------------------|---|
| Power System | 4 Electric Motors (Li-Polymer Battery) |
| Number of Seats | 1 |
| Cruise Speed | 110 km/h |
| Maximum Engine Power | 22 KW |
| Maximum Speed | 210 km/h |
| Maximum Endurance | 30 min |

3.4 PIPISTREL TAURUS G2

The design of Pipistrel Taurus G2 is shown in Figure 6. The specifications of the aircraft are given in Table 6.



Figure 6. Pipistrel Taurus G2 [18].

Table 6. Pipistrel Taurus G2 Specifications.

| | |
|----------------------|-----------------------------|
| Power System | Electric Motor (Battery) |
| Number of Seats | 1 |
| Cruise Speed | 110 km/h |
| Maximum Engine Power | 40 KW |
| Maximum Range | 200 km |
| Maximum Endurance | 2 h |

3.5 PIPISTREL PANTHERA

The design of Pipistrel Panthera is shown in Figure 7. The specifications of the aircraft are given in Table 7.



Figure 7. Pipistrel Panthera [19].

Table 7. Pipistrel Panthera Specifications.

| | |
|----------------------|-----------------------------|
| Power System | Electric Motor (Battery) |
| Number of Seats | 4 |
| Cruise Speed | 218 km/h |
| Maximum Engine Power | 145 KW |
| Maximum Range | 400 km |
| Service Ceiling | 4000 m |

3.6 ANTARES H3

The design of Antares H3 is shown in Figure 8. The specifications of the aircraft are given in Table 8.

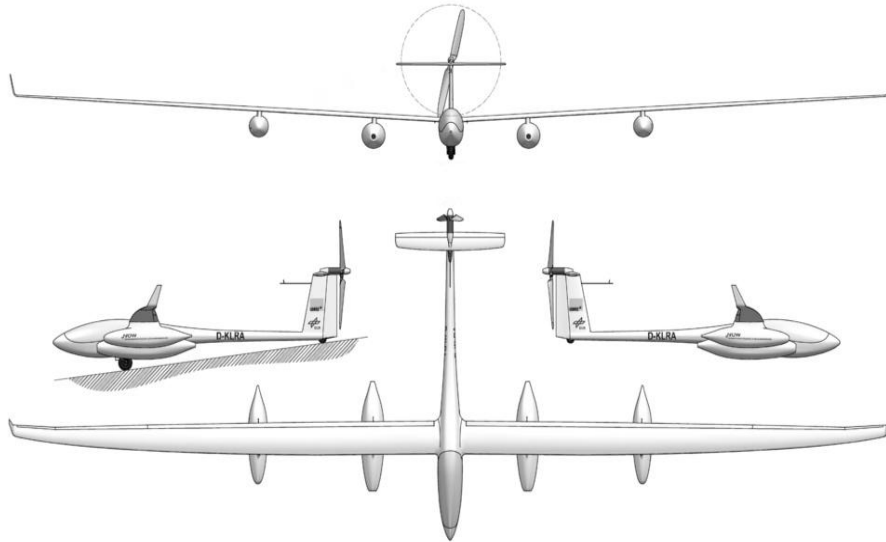


Figure 8. Antares H3 [9].

Table 8. Antares H3 Specifications.

| | |
|----------------------|-------------------------------|
| Power System | Electric Motor (Fuel Cell) |
| Operation | UAV |
| Maximum Speed | 250 km/h |
| Maximum Engine Power | 36 KW |
| Maximum Range | >6000 km |
| Maximum Endurance | >50 h |

4.0 DESIGN REQUIREMENTS

The design requirements for the proposed aircraft are as follows.

- General aviation, FAR 23 certifiable
- 4 passengers (including pilot)
- Electrically powered
- Range = 800 km
- Cruise speed = 200 km / h

5.0 PROPULSION TYPE SELECTION

The following factors are taken into consideration in the selection of the propulsion system:

1. Power density
2. Energy density
3. Safety
4. Cost
5. Reliability

A trade study was performed to decide the type of energy source, namely a battery or a fuel cell. The battery and fuel cell characteristics needed to produce 135 hp in a ground based electric vehicle are shown in Tables 9 and 10 [13]. Based on this comparison, the best option is the battery due to its lower weight, volume, and cost. Although the energy density of the fuel cell is higher than that of the battery, the space occupied by the fuel cell is too large to be used in a 4 seat aircraft.

Table 9. Fuel Cell Specifications.

| Component | Weight (Kg) | Volume (Liters) | Cost (\$) |
|------------------------|-------------|-----------------|-----------|
| Fuel Tank | 617 | 1182 | 23,033 |
| 3.2 kg Storage Tank | 51 | 215 | 2,288 |
| Drive Train | 53 | 68 | 3,826 |
| Total | 721 | 1465 | 29,147 |

Table 10. Battery Specifications.

| Component | Weight (Kg) | Volume (Liters) | Cost (\$) |
|----------------|-------------|-----------------|-----------|
| Li ion Battery | 451 | 401 | 16,125 |
| Drive Train | 53 | 68 | 3,826 |
| Total | 504 | 469 | 19,951 |

The following sections explain the characteristics of motor and battery selection.
The lightest and most efficient devices have been chosen for the proposed design.

5.1 ELECTRIC MOTOR CHARACTERISTICS

A DC brushless motor is chosen because of its higher reliability and higher torque at lower rpm. The brushless motor is purely inductive. Unlike a brushed motor, there is no brush to replace, so the motor life depends mostly on the bearings.

5.2 PROPELLER CHARACTERISTICS

The desired characteristics of the propeller are for light weight and low noise production for the desired level of thrust. Increasing the number of blades decreases noise, but it also increases the structural weight and decreases blade efficiency. Each blade rotates in the wake of a closely positioned blade as the number of blades increases. Decreasing the number of blades requires a larger diameter for the propeller, which increases noise, as the propeller tip rotates at higher speeds and reduces the ground clearance. Based on these considerations, a propeller with three blades is chosen for the proposed design.

The diameter of the propeller is obtained from the following equation [10]:

$$D_p = \left(\frac{4P_{max}}{\Pi n_p P_{bl}} \right)^{0.5} \quad (1)$$

where

D_p - propeller diameter ft

P_{bl} - power loading per blade hp/ft²

n_p - number of blades

P_{max} - maximum engine power hp

$$P_{bl} = 3.2$$

$$P_{max} = 203.5 \text{ HP}$$

$$n_p = 3$$

$$D_p = 5.2 \text{ ft}$$

5.3 BATTERY CHARACTERISTICS

The battery source is selected based on the specific energy, specific power and operating voltage range of the battery. Table 11 shows different battery types. Based on this comparison, the Li-Po battery seems to offer all of the desirable characteristics for the proposed airplane [14].

Table 11. Comparison of Different Batteries.

| Battery | Theoretical Specific Energy (W-h/kg) | Practical Specific Energy(W-h/kg) | Specific Power(W/kg) | Cell Voltage(V) |
|---------|--------------------------------------|-----------------------------------|----------------------|------------------|
| Pb/acid | 170 | 50 | 180 | 1.2 |
| Ni/Cd | 240 | 60 | 150 | 1.2 |
| NiMH | 470 | 85 | 400 | 1.2 |
| Li-ion | 700 | 135 | 340 | 3.6 |
| Li-Po | 735 | 220 | 1900 | 3.7 |
| LiS | 2550 | 350 | 700 | 2.5 |

6.0 PRELIMINARY SIZING

The preliminary sizing of the aircraft is performed following the steps in reference [10].

6.1 TAKEOFF WEIGHT ESTIMATION

The takeoff weight is subdivided into different groups as shown below. A general idea of the weight of each group is obtained from existing electric aircraft, such as the Taurus G4, the Diamond DA40, and the Cessna Corvalis TTX.

$$W_{TO} = W_E + W_P + W_B + W_{PL} \quad (2)$$

W_{TO} = Takeoff weight

W_E = Empty weight (structures, avionics, etc.)

W_P = Propulsion system weight (propeller, motor, motor controller)

W_B = Battery weight

W_{PL} = Payload

Using data from existing electric aircraft for guidance, these weights are estimated as follows:

$W_E = 750$ kg

$W_P = 100$ kg

$W_{PL} = 400$ kg (each passenger: 75 kg + 25 kg for luggage)

$W_B = 500$ kg

Hence, $W_{TO} = 1750$ kg.

6.2 PERFORMANCE SIZING

The design point is obtained from the performance sizing graph. The aircraft is sized according to the FAR 23 requirements.

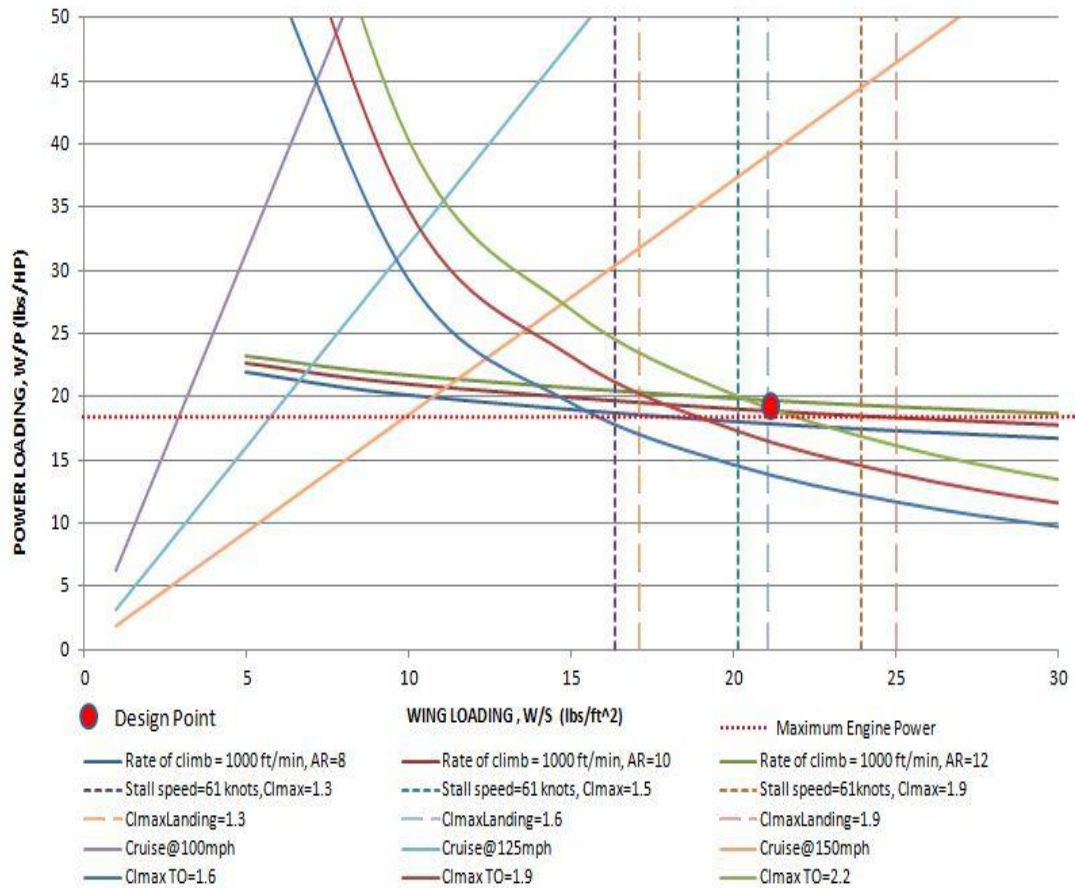


Figure 9. Performance Sizing Graph.

6.3 SUMMARY OF PERFORMANCE SIZING

The design point chosen is shown on the performance sizing graph. Table 12 provides the summary of performance sizing.

Table 12. Summary of Performance Sizing.

| | |
|-----------------------|-------------------------|
| Stall Speed | 61 Knots |
| Rate of Climb | 1000 ft/min |
| $C_{l, \max TO}$ | 2.2 |
| $C_{l, \max L}$ | 1.6 |
| Aspect Ratio | 10 |
| Takeoff Wing Loading | 21 lb / ft ² |
| Takeoff Power Loading | 19 lb / hp |
| Wing Span | 43 ft |
| Chord | 4.3 m |
| Engine Power | 203 hp |

6.4 BATTERY SIZING

The battery is sized following the method in reference [14]. The thrust power generated by the propeller is:

$$P_{Thrust} = T \cdot V \quad (3)$$

For level, unaccelerated flight, thrust equals drag. Hence,

$$P_{Thrust} = D \cdot V = \frac{W_{TO}}{\frac{L}{D}} \cdot V \quad (4)$$

The energy needed from the battery is:

$$E = \frac{E_B}{P_B} \quad (5)$$

where,

E = Endurance of flight

E_B = Battery Energy

P_B = Battery Power

$$1 \text{ KWH} = 3.6 * 10^6 \text{ J}$$

The specific energy (KWh) is found out using the above conversion method. The mass of the battery is estimated using the specific energy of Li-Po battery. Tables 13 and 14 show the thrust power, specific energy and battery mass battery required for different L/D ratios and cruise velocities. The endurance changes as a function of cruise speed. A 30-minute reserve has been taken into account. The mass of the battery is calculated based on the theoretical specific energy of the battery.

Table 13. Effect of L/D over Thrust Power and Battery Energy.

| L/D | Thrust Power(KW) | | | Battery Energy(MJ) | | |
|-----|------------------|-----------|-----------|--------------------|-----------|-----------|
| | V=150Km/h | V=200Km/h | V=250Km/h | V=150 Km/h | V=200Km/h | V=250Km/h |
| 13 | 73 | 96.9 | 121.2 | 1525.6 | 1570.1 | 1613.7 |
| 14 | 67.5 | 90 | 112.5 | 1416.7 | 1458 | 1498.5 |
| 15 | 63 | 84 | 105 | 1322.2 | 1360.8 | 1398.6 |
| 16 | 59 | 78.7 | 98.4 | 1239.6 | 1275.7 | 1311.1 |
| 17 | 55.6 | 74.1 | 92.6 | 1166.7 | 1200.7 | 1234.1 |
| 18 | 52.5 | 70 | 87.5 | 1101.8 | 1134 | 1165.5 |
| 19 | 49.7 | 66.3 | 82.8 | 1043.8 | 1074.3 | 1104.1 |
| 20 | 47.3 | 63 | 78.7 | 991.6 | 1020.6 | 1048.9 |
| 21 | 45 | 60 | 75 | 944.4 | 972 | 999 |
| 22 | 42.9 | 57.3 | 71.6 | 901.5 | 927.8 | 953.5 |
| 23 | 41.1 | 54.8 | 68.5 | 862.3 | 887.4 | 912.1 |
| 24 | 39.4 | 52.5 | 65.6 | 826.4 | 850.5 | 874.1 |
| 25 | 37.8 | 50.4 | 63 | 793.3 | 816.4 | 839.1 |

Table 14. Effect of L/D over Specific Energy and Battery Mass.

| L/D | Specific Energy(KW-hr) | | | Battery Mass (Kg) | | |
|-----|------------------------|-----------|-----------|-------------------|-----------|-----------|
| | V=150Km/h | V=200Km/h | V=250Km/h | V=150 Km/h | V=200Km/h | V=250Km/h |
| 13 | 423.7 | 436.1 | 448.2 | 576.5 | 593.4 | 609.8 |
| 14 | 393.5 | 405 | 416.2 | 535.4 | 551.1 | 566.3 |
| 15 | 367.2 | 378 | 388.5 | 499.7 | 514.3 | 528.5 |
| 16 | 344.3 | 354.3 | 364.2 | 468.4 | 482.1 | 495.5 |
| 17 | 324.1 | 333.5 | 342.7 | 440.9 | 453.7 | 466.3 |
| 18 | 306.1 | 315 | 323.7 | 416.4 | 428.5 | 440.4 |
| 19 | 289.9 | 298.4 | 306.7 | 394.5 | 406.1 | 417.3 |
| 20 | 275.4 | 283.5 | 291.3 | 374.7 | 385.7 | 396.4 |
| 21 | 262.3 | 270 | 277.5 | 356.9 | 367.3 | 377.5 |
| 22 | 250.4 | 257.7 | 264.8 | 340.7 | 350.6 | 360.4 |
| 23 | 239.5 | 246.5 | 253.3 | 325.9 | 335.4 | 344.7 |
| 24 | 229.5 | 236.2 | 242.8 | 312.3 | 321.4 | 330.5 |
| 25 | 220.3 | 226.8 | 233.1 | 299.8 | 308.5 | 317.1 |

It is clear from Table 14 that a L/D ratio of 16 or above is required at a cruise velocity of 200 km/h to achieve a battery mass of no more than 500 kg, as estimated in the preliminary weight sizing earlier.

7.0 PRELIMINARY DESIGN

7.1 FUSELAGE LAYOUT

The fuselage is sized to provide adequate space for four passengers and their baggage. The method in reference [10] is used to decide on the values of the various fuselage parameters.

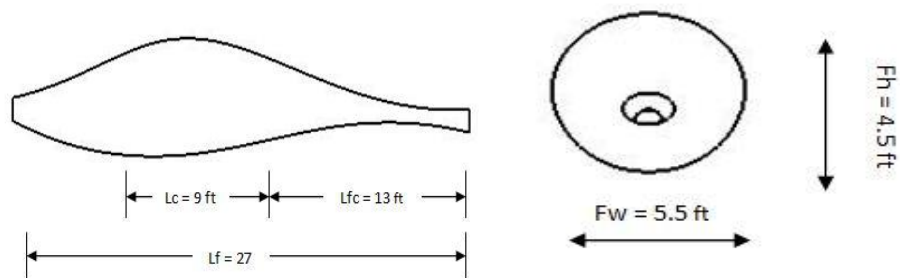


Figure 10. Fuselage Dimensions.

Fuselage Diameter = 4.5 ft

Fuselage Length = 27 ft

Tail Cone Length = 13.5 ft

Cabin Dimensions:

Maximum Height = 4.5 ft

Maximum Width = 5.5 ft

Maximum Length = 9 ft

7.2 ENGINE SELECTION AND DISPOSITION

To provide a clean flow over the wings, a fuselage-mounted single engine is chosen. An electric motor with an output power of 160 KW and a 3-blade propeller with a diameter of 5.2 ft are selected. The engine location is shown in Figure 11.

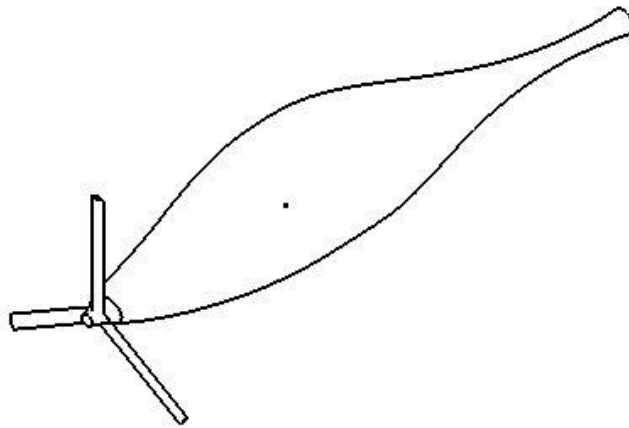


Figure 11. Nose Mounted Engine.

7.3 WING DESIGN

A cantilever, low wing is selected for the design due to its favourable ground effect during takeoff and the shorter landing gear, which helps in reducing the structural weight. Also, the wings can be used as a step to enter into the aircraft. From the summary of the performance sizing results, the wing specifications can be calculated:

Wing Area, $S = 184 \text{ ft}^2$

Aspect Ratio, $AR = 10$

Wing Span, $b = 43 \text{ ft}$

Chord, $c = 4.3$ ft

From the existing data of similar aircraft using [10], the other wing parameters such as taper ratio, dihedral angle, sweep angle, twist angle, and incidence angle are also obtained.

Taper ratio = 0.4

Dihedral = 7°

Sweep = 0°

Wing twist = -3°

Incidence angle = 2°

From reference [13],

$$\bar{c} = \frac{2}{3} C_r \left(\frac{1 + \lambda + \lambda^2}{1 + \lambda} \right) \quad (6)$$

where,

\bar{c} = mean aerodynamic chord = 4.3 ft

λ = taper ratio = 0.4

c_r = root chord = 5.78 ft

c_t = tip chord = 2.31 ft

To find the flap dimensions, the following approximation is used:

$c_f / c = 0.2$

$b_f / b = 0.7$

Hence, the flap dimensions are:

$$c_f = 0.86 \text{ ft}$$

$$b_f = 30 \text{ ft}$$

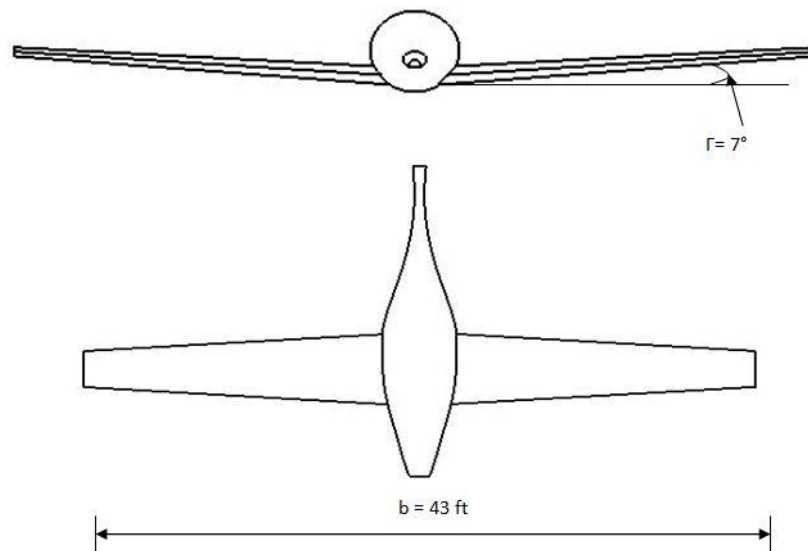


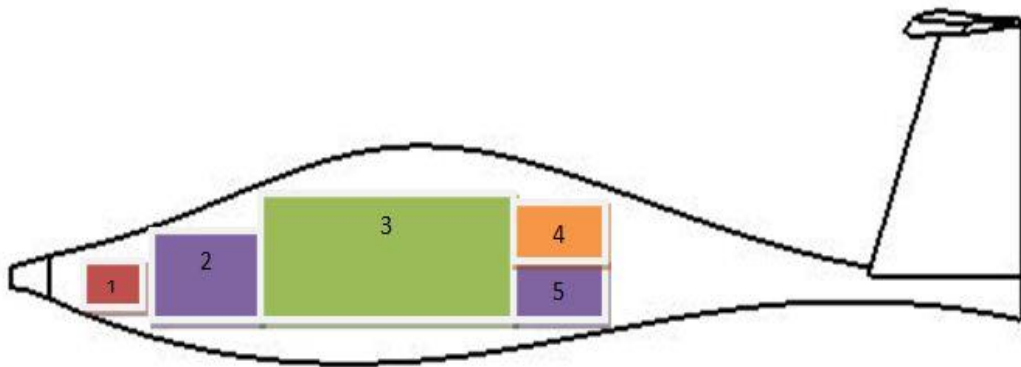
Figure 12. Wing specifications.

7.4 WEIGHT AND BALANCE ANALYSIS

The various components that contribute to the aircraft weight are shown in Figure 13 for the purpose of estimating the aircraft cg. Table 15 shows an estimation of the empty weight cg at 10 ft from the nose of the fuselage using data from existing aircraft [10], while Table 16 gives the location of the aircraft cg.

Table 15. Estimation of Empty Weight CG.

| Component | Weight (kg) | X (m) |
|-------------------|-------------|-------|
| Wings | 265 | 2.56 |
| Empennage | 65 | 7.62 |
| Fuselage | 250 | 2.46 |
| Nose Landing Gear | 20 | 1.83 |
| Main Landing Gear | 100 | 2.54 |



- 1 - Motor + Controller
- 2 - Battery
- 3 - Passengers
- 4 - Baggage
- 5 - Battery

Figure 13. Location of Various Components for Estimating the CG Location.

Table 16. CG Estimation.

| Component | Weight (kg) | x (m) |
|----------------|-------------|-------|
| Propulsor Unit | 100 | 0.15 |
| Battery | 350 | 1.06 |
| Passengers | 300 | 2.89 |
| Empty Weight | 750 | 3.04 |
| Baggage | 100 | 4.72 |
| Battery | 150 | 4.72 |

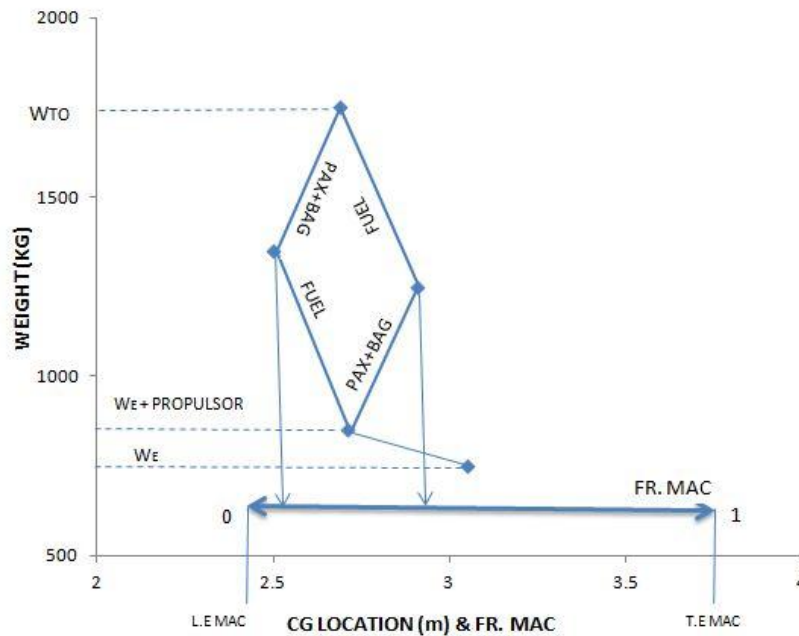


Figure 14. CG Excursion Diagram.

From Figure 14, the cg travel of the aircraft is 16 in or 31% of the wing mean aerodynamic chord.

7.5 LANDING GEAR

A retractable, conventional, tricycle landing gear is chosen to reduce drag and to provide the greatest extent of laminar flow over the wing during cruise. The landing gear specifications and location are determined by the ground clearance and tip over criteria [10]. To provide adequate clearance for the propeller, the length of the nose landing gear is chosen at 4 ft and the length of the main landing gear at 3 ft.

The nose gear is placed 86 inches from the nose of the fuselage, while the main gear is located 125 inches of the fuselage section. The static load per strut for the nose and main landing gears is found from:

$$\frac{P_n}{W_{to}} = 0.25 \quad (7)$$

$$\frac{2P_m}{W_{to}} = 0.74$$

From equation (7) and typical landing gear wheel data [10], the landing gear specifications are easily obtained.

7.6 EMPENNAGE

A T-tail is chosen for the proposed design because it provides the best location for staying out of the wing wake and it increases the efficiency of the horizontal stabilizer, thus requiring a smaller area. From the configuration layout, the distance of the horizontal and the vertical stabilizer from the cg is obtained:

$$x_h = 15 \text{ ft,}$$

$$x_v = 14.5 \text{ ft}$$

Hence

$$S_h = 32.2 \text{ ft}^2, \quad S_v = 20.2 \text{ ft}^2$$

$$b_h = 12.7 \text{ ft}, \quad b_v = 30.3 \text{ ft}$$

$$c_h = 2.54 \text{ ft}; \quad c_v = 3.7 \text{ ft}$$

A taper ratio of 0.5 is chosen on both the horizontal and the vertical stabilizers based on data from similar aircraft [10].

7.7 HIGH LIFT DEVICES

A plain flap is the most simple high lift device which provides a maximum increment of 0.9 while adding less structural weight. Hence a plain flap is chosen in this design. Table 17 gives the increment in lift coefficient for each device [13].

Table 17. Lift Coefficient Increments for Various Types of High Lift Devices.

| High Lift Device | ΔC_l |
|---------------------|--------------|
| Plain Flap | 0.7-0.9 |
| Split Flap | 0.7-0.9 |
| Fowler Flap | 1-1.3 |
| Slotted Flap | 1.3 Cf/C |
| Double Slotted Flap | 1.6 Cf/C |
| Triple Slotted Flap | 1.9 Cf/C |
| Leading Edge Flap | 0.2-0.3 |

| | |
|-------------------|---------|
| Leading Edge Slat | 0.3-0.4 |
| Kruger Flap | 0.3-0.4 |

7.8 AIRFOIL SELECTION

The ideal and maximum lift coefficients for the airfoil are calculated from the equations in reference [13]:

$$C_{l_{ideal}} = 0.8$$

$$C_{l_{max}} = 1.4$$

The airfoil is chosen primarily based on these two criteria. The ideal lift coefficient is higher when compared to the average ideal lift coefficient, which is usually in the range of 0.2 – 0.4. Hence, the induced drag produced by the wing will be higher, but the Pipistrel Panthera has an ideal lift coefficient of 0.7, which is comparable. The airfoils that have the highest ideal lift coefficient are considered to find the best suitable one.

The NACA 6-series airfoils have high ideal lift coefficient [13]. A number of airfoils were selected and their lift, drag, and pitching moment characteristics are compared in Figures 15 through 20, to find the best airfoil. From the results, two airfoils, NACA 65618 and NACA 66212 were selected and compared. The NACA 65618 generated high lift-to-drag ratios during cruise and a smaller pitching moment coefficient, hence it is chosen for the proposed design.

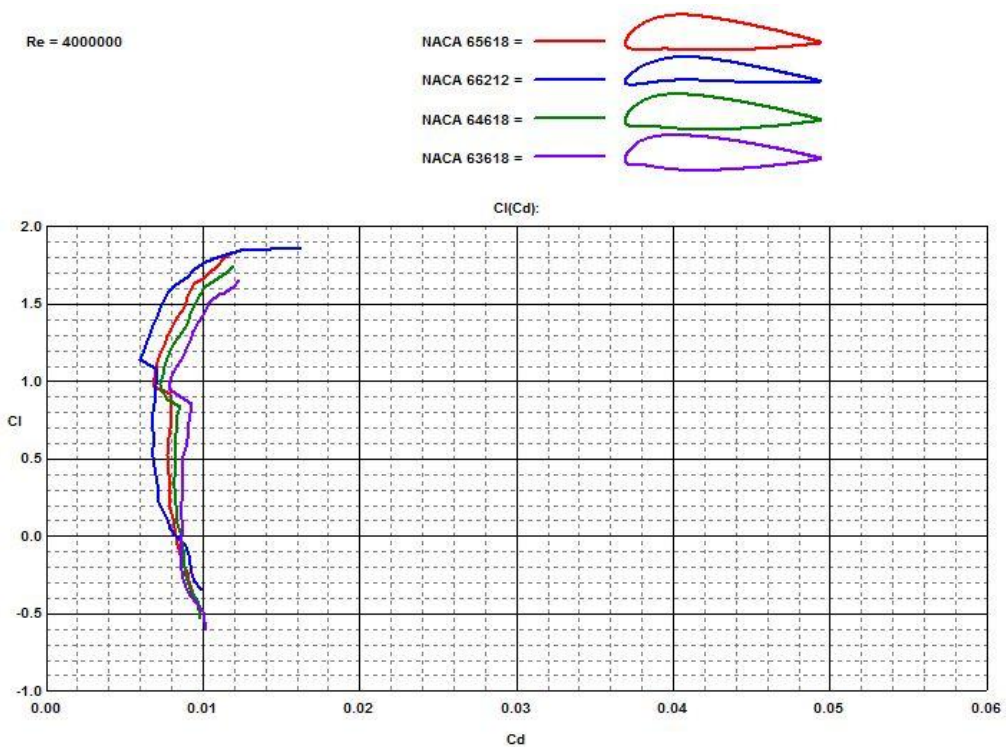


Figure 15. Drag Polar Comparison of Various Naca 6-Series Airfoils.

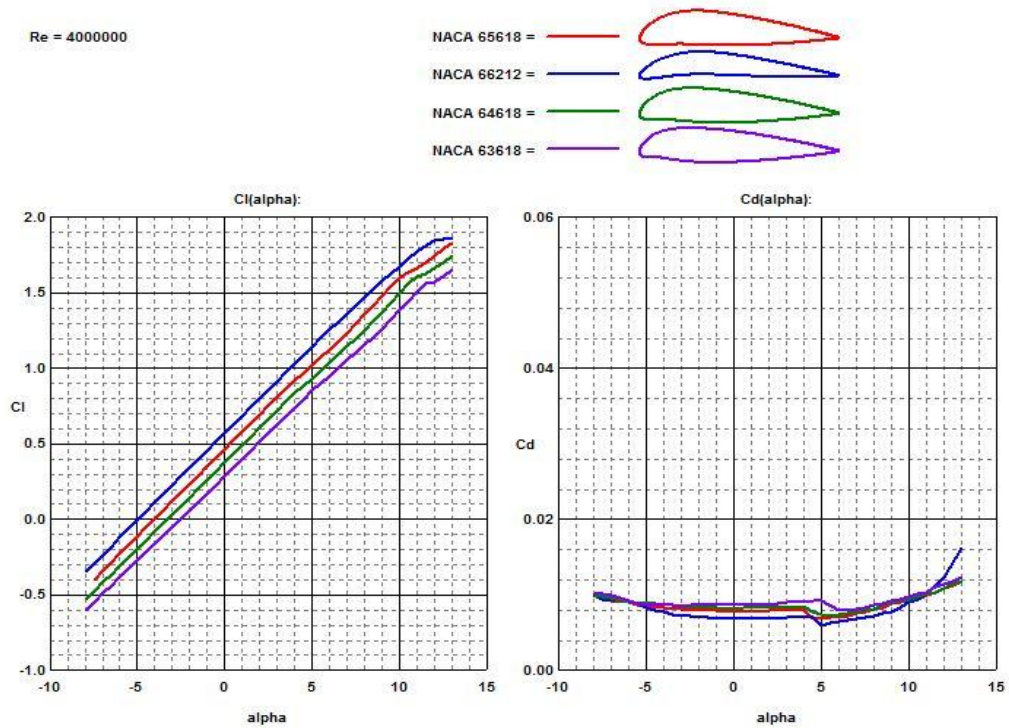


Figure 16. Lift and Drag Characteristics Comparison of Various Naca 6-Series Airfoils.

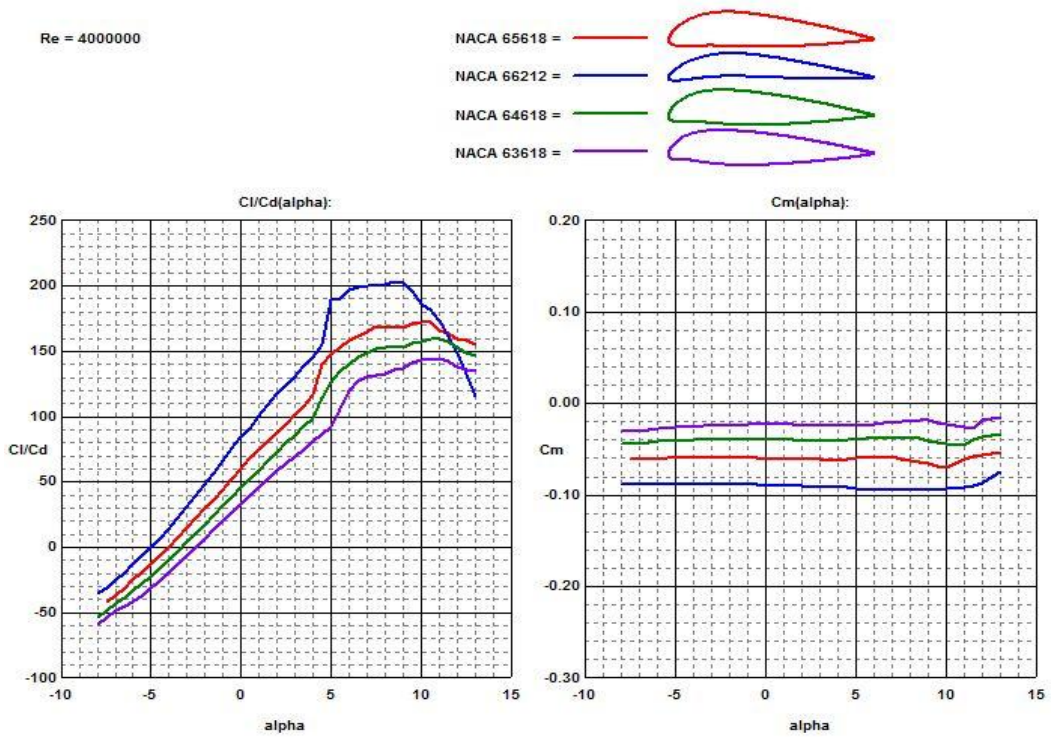


Figure 17. Lift-To-Drag Ratio and Pitching Moment Comparison of Various Naca 6-Series Airfoils

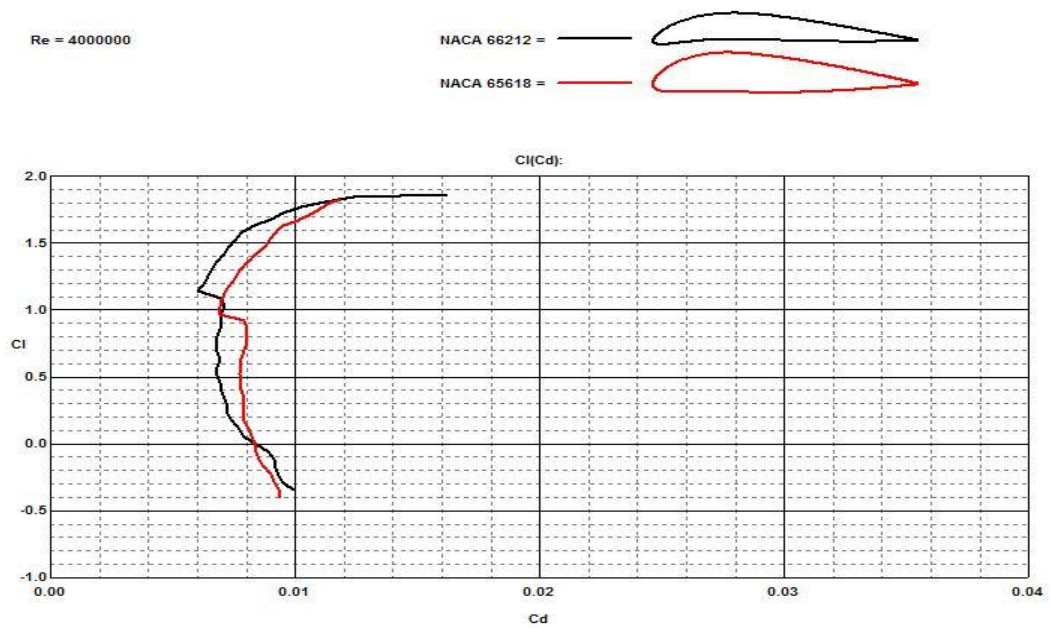


Figure 18. Comparison of the Drag Polars for the Naca 66212 and Naca 65618 Airfoils.

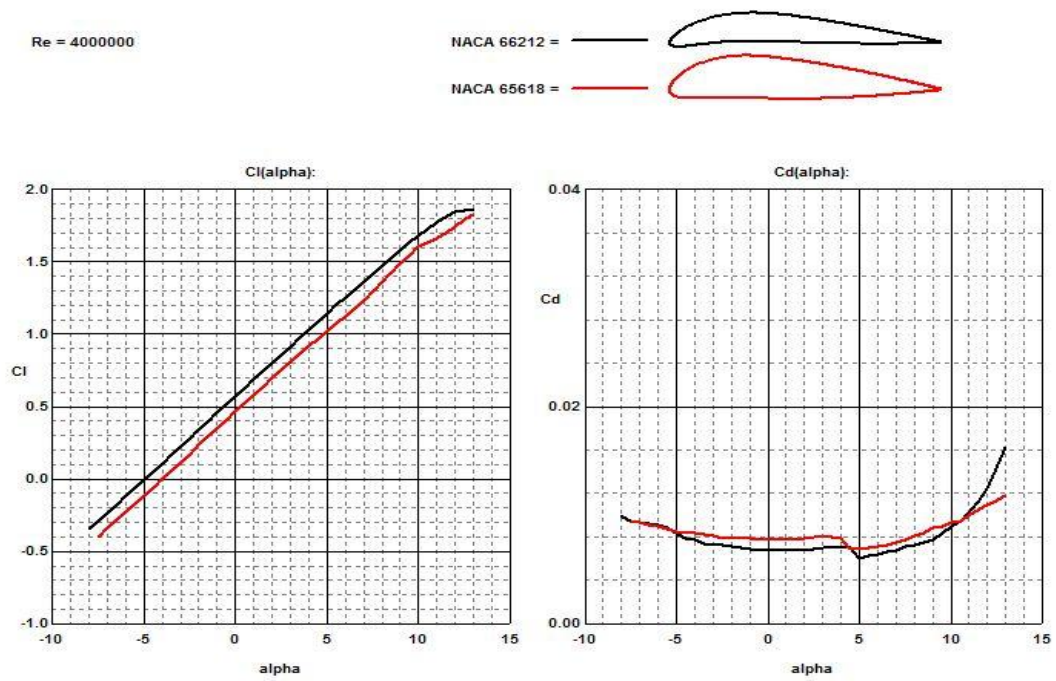


Figure 19. Comparison of the Lift and Drag of the Naca 66212 and Naca 65618 Airfoils.

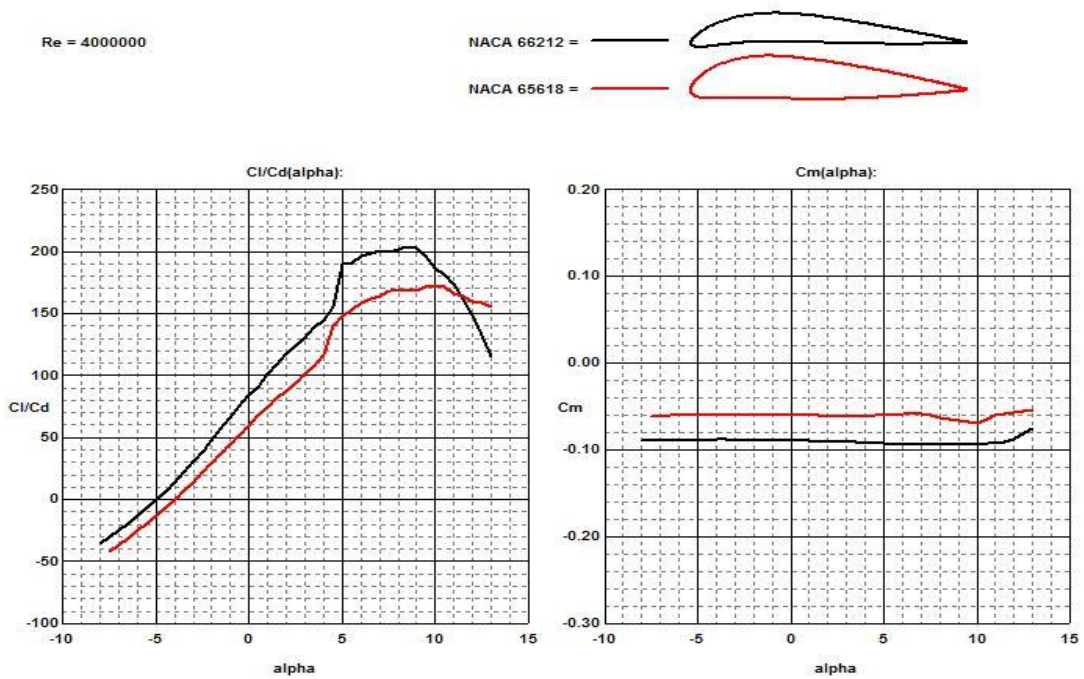


Figure 20. Comparison of the L/D Ratio and Moment of the Naca 66212 and Naca 65618 Airfoils.

7.9 DRAG POLAR

The preliminary estimates of the airplane low-speed drag coefficient and Oswald efficiency factor are estimated for different configurations of the aircraft and shown in Table 18 [10].

Table 18. Preliminary Estimates of C_{D_0} and e .

| Configuration | C_{D_0} | E |
|---------------|-------------|-----------|
| Clean | 0 | 0.80-0.85 |
| Takeoff Flaps | 0.010-0.020 | 0.75-0.80 |
| Landing Flaps | 0.055-0.075 | 0.70-0.75 |
| Landing gear | 0.015-0.025 | No effect |

The wetted surface area of the aircraft is estimated to be $S_{wet} = 676 \text{ ft}^2$, while the equivalent parasite area is estimated at $f = 4$. Hence:

$$C_{D_0} = \frac{f}{S} \quad (8)$$

$$C_{D_0} = 0.02$$

$$C_D = C_{D_0} + \frac{C_l^2}{\pi A e} \quad (9)$$

Table 19. Drag Coefficient and L/D Ratio for Different Aircraft Configurations.

| Configuration | C_D | C_l | L/D |
|--------------------|-------|-------|-----|
| Clean | 0.044 | 0.8 | 18 |
| Take off, gear up | 0.22 | 2.2 | 10 |
| Takeoff, gear down | 0.24 | 2.2 | 9 |
| Landing, gear up | 0.18 | 1.6 | 8.7 |
| Landing, gear down | 0.19 | 1.6 | 8 |

$$\left(\frac{L}{D}\right)_{max} = 18$$

This value for $(L/D)_{max}$ obtained from the drag polar satisfies the initial estimate of the battery mass, as shown earlier in Table 14, hence, no iteration is needed.

10.0 PRELIMINARY DESIGN LAYOUT

Figure 21 shows the preliminary design layout of the proposed 4-seat, general aviation, electric aircraft.

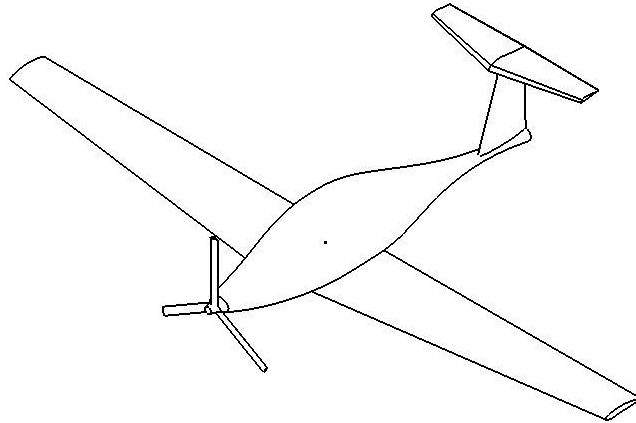


Figure 21. Preliminary Design Layout.

Figure 22 shows the three views of the proposed electric aircraft.

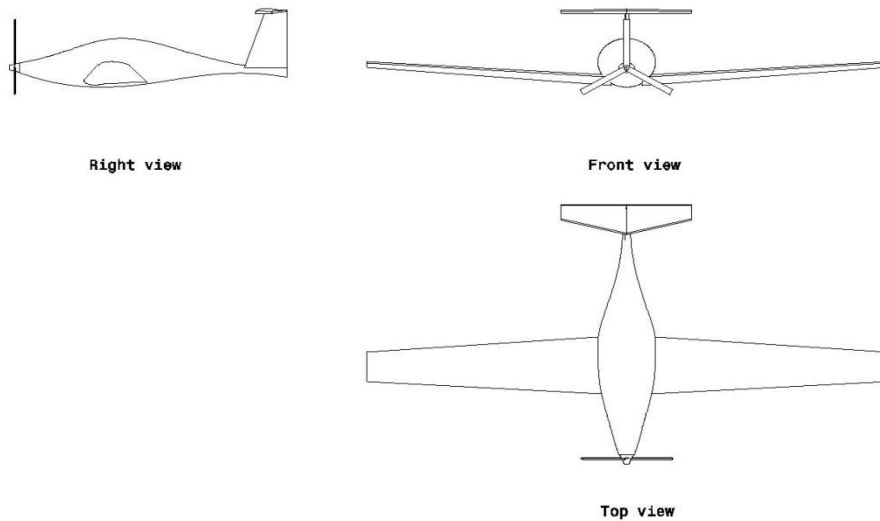


Figure 22. Electric Aircraft: Three View.

11.0 CONCLUSION

It is noted that the range and efficiency of the electric aircraft depend heavily on the takeoff weight. The takeoff weight of 1,750 kg is much higher when compared to aircraft of the same category such as, for example, the Pipistrel Panthera, which has a takeoff weight of 1,200 kg. This, of course, is due to the higher L/D ratio, which reduces the energy needed during flight, and as a consequence, the required battery weight. Needless to say, the proposed design extrapolates on advances in battery technology, composite structures, and aerodynamics to help achieve the performance shown in this thesis. The next step is a detailed analysis of each subsystem to confirm the feasibility of the proposed concept.

REFERENCES

- [1] Epstein, Aircraft propulsion, presented at NASA ARC green aviation workshop, Mountain View, April 2009.
- [2] G.L. Dillingham, Aviation and the Environment, United States Government Accountability Office, 2008.
- [3] CAFE: Electric aircraft symposium report, 2010. Retrieved from <<http://www.youtube.com/watch?feature=endscreen&NR=1&v=d24knbykgVo>>
- [4] Aero-tv: Bye energy's electric 172 - building a greener future for aviation, 2011. Viewed at <http://www.youtube.com/watch?v=Yjq8ixM0oEw>
- [5] D. Yoney, Cessna Developing Electric-Powered 172 Skyhawk, 2010. Retrieved from <<http://green.autoblog.com/2010/08/11/cessna-developing-electric-powered-172-skyhawk/>>
- [6] J. Croft, Electric Propulsion is Gaining Horsepower with Experimental and Light Aircraft Communities, Aug. 02, 2010. Retrieved from <<http://www.flightglobal.com/news/articles/electric-propulsion-is-gaining-horsepower-with-experimental-and-light-aircraft-communities-345516>>
- [7] R. Coppinger, The Future is Electric for General Aviation, Apr 06, 2010. Retrieved from <<http://www.flightglobal.com/news/articles/the-future-is-electric-for-general-aviation-340170>>
- [8] Electric Aircraft, Mar. 09, 2012. Retrieved from http://en.wikipedia.org/wiki/Electric_aircraft
- [9] Antares H2/H3 Technical Data. Retrieved from http://www.lange-aviation.com/htm/english/products/antares_h3/technical_data.html
- [10] J. Roskam, Airplane Design vol I - Preliminary Sizing of Airplanes, 1985.
- [11] K. Loftin, Subsonic Aircraft: Evolution and the Matching of Size to Performance. NASA Reference Publication 1060.
- [12] M. Sadraey, Aircraft Design: A Systems Engineering Approach. Wiley, 2012.
- [13] E. Stephen, E. James, E. A Cost Comparison of Fuel-Cell and Battery Electric Vehicles.
- [14] J. Gundlach, Designing unmanned aircraft systems, 2012. Retrieved from <<http://arc.aiaa.org/doi/book/10.2514/4.868443>>

- [15] Wong, G. (2011, March 03). Elektra one: the electricity-powered plane. Retrieved from <http://www.ubergizmo.com/2011/03/elektra-one/>
- [16] Hanlon, M. (2009, June 22). Retrieved from <http://www.gizmag.com/yuneec-e430-electric-aircraft/12036/>
- [17] 4-engine electric cri-cri unveiled by eads. (n.d.). Retrieved from http://www.eaa.org/news/2010/2010-06-24_cri-cri.asp
- [18] (2011, Feb 26). Retrieved from <http://www.technologicvehicles.com/en/green-transportation-news/569/video-the-electric-self-launching-glider-pipi>
- [19] (2012, Apr 19). Retrieved from <http://www.ecofriend.com/pipistrel-panthera-ultra-sleek-aircraft-electric-hybrid-cousins-down-line.html>